SHELLOCK
R & D SERVICES, INC.

7511 McConnell Avenue
Los Angeles, CA 90045
(310) 670-7095 voice (310) 417-8639 fax
www.MagneticResonanceSafetyTesting.com

REPORT
Evaluation of Magnetic Resonance (MR) Safety for Five Different Markers

Project Conducted by:
Frank G. Shellock, Ph.D.
Shellock R & D Services, Inc.
7511 McConnell Ave.
Los Angeles, CA 90045

11/25/04

Presented to:
Bob Johnson
Carbon Medical Technologies, Inc.,
1290 Hammond Rd.
White Bear Lake, MN 55110

For medical implants and devices, the objectives of magnetic resonance (MR) safety testing are to determine the presence of magnetic field interactions and heating for implants and devices in association with the use of an MR system. Accordingly, MR safety tests were conducted at 3-Tesla on the following objects:

DEVICE	MATERIAL	SIZE	APPLICATION
Test Article 1	Carbon coated zirc. Oxide	0.121 x 0.054 inch	Breast Tumor Marking
Test Article 2	Carbon coated zirc. Oxide	0.121 x 0.054 inch	Breast Tumor Marking
Test Article 3	Carbon coated zirc. Oxide	0.182 x 0.079 inch	Breast Tumor Marking
Test Article 4	Carbon coated zirc. Oxide	0.182 x 0.079 inch	Breast Tumor Marking
Control 1	Titanium alloy	0.080 x 0.050 inch	Breast Tumor Marking

In addition, artifacts were characterized for these five markers at 3-Tesla.

The term "MR-safe" is defined by the American Society for Testing and Materials (ASTM) Designation: F 2052. Standard test method for measurement of magnetically induced displacement force on passive implants in the magnetic resonance environment. In: Annual Book of ASTM Standards, Section 13, Medical Devices and Services, Volume 13.01 Medical Devices; Emergency Medical Services. West Conshohocken, PA, pp; 1576-1580, 2001, as follows:

“MR-safe: The device, when used in the MR environment, has been demonstrated to present no additional risk to the patient or other individuals, but may affect the quality of the diagnostic information. Importantly, the specific conditions used for assessment of MR safety must be specified.”

MAGNETIC FIELD INTERACTIONS

Testing for magnetic field interactions involved evaluations of translational attraction and torque for the five different markers using a 3-Tesla MR system (General Electric Medical Systems, Milwaukee, WI).

Translational Attraction

For the assessment of translational attraction (that is, the displacement force), a test was conducted known as the “deflection angle test”, which is described in the following publications:

(1) American Society for Testing and Materials (ASTM) Designation: F 2052. Standard test method for measurement of magnetically induced displacement force on passive implants in the magnetic resonance environment. In: Annual Book of ASTM Standards, Section 13, Medical Devices and Services, Volume 13.01 Medical Devices; Emergency Medical Services. West Conshohocken, PA, pp; 1576-1580.
(2) Shellock FG, Morisoli SM. Ex vivo evaluation of ferromagnetism, heating, and artifacts for heart valve prostheses exposed to a 1.5 Tesla MR system. Journal of Magnetic Resonance Imaging. 4:756-758, 1994.
(3) Shellock FG, Morisoli SM. Ex vivo evaluation of ferromagnetism and artifacts for cardiac occluders exposed to a 1.5 Tesla MR system. Journal of Magnetic Resonance Imaging, 4:213-215, 1994.
(4) Shellock FG, Detrick MS, Brant-Zawadski M. MR-compatibility of Guglielmi detachable coils. Radiology. 203: 568-570, 1997.
(5) Edwards, M-B, Taylor KM, Shellock FG. Prosthetic heart valves: evaluation of magnetic field interactions, heating, and artifacts at 1.5 Tesla. Journal of Magnetic Resonance Imaging. 12:363-369, 2000.
(6) Shellock FG, Shellock VJ. Stents: Evaluation of MRI safety. American Journal of Roentgenology. 173:543-546, 1999.
(7) Shellock FG. Surgical instruments for interventional MRI procedures: assessment of MR safety. Journal of Magnetic Resonance Imaging, 13:152-157, 2001.
(8) Shellock FG. Biomedical implants and devices: assessment of magnetic field interactions with a 3.0-Tesla MR system. Journal of Magnetic Resonance Imaging. 16:721-732, 2002.

The American Society for Testing and Materials (ASTM) Designation: F 2052. Standard test method for measurement of magnetically induced displacement force on passive implants in the magnetic resonance environment was carefully followed for this test.

Each marker was attached to a special test fixture to measure the deflection angle in the MR system. The test fixture consisted of a sturdy structure capable of holding each marker in position without movement of the test fixture and contained a protractor with 1˚-graduated markings, rigidly mounted to the structure. The 0˚ indicator on the protractor was oriented vertically. The test fixture also had a plastic bubble level device attached to the top to ensure proper orientation in the MR system during the test procedure. Sources of forced air movement within the MR system bore were turned off during the measurements.

Each marker was suspended from a thin, lightweight string that was attached at the 0˚ indicator position on the protractor. The length of the string was 20-cm, which was long enough so that marker could be suspended from the test fixture and hang freely in space. Motion of the string with the marker was not constrained by the support structure of the protractor.

Measurements of deflection angles for the markers were obtained at the position in the 3-Tesla MR system that produced the greatest magnetically induced deflection. This point was determined for the MR system using gauss line plots, measurements, and visual inspection to identify the location where the spatial magnetic field gradient was the greatest. The location was marked by tape to facilitate measurements of the deflection angles for the markers.

The direction of the magnetic field for the 3-Tesla scanner is horizontal. The highest spatial gradient for the 3-Tesla MR system (Excite, General Electric Medical Systems, Milwaukee, WI) occurs at a position that is 74-cm from isocenter of the scanner. The magnetic spatial gradient at this position is 720 gauss/cm (Personal Communication, Dewain Purgill and Daniel J. Schaefer, General Electric Medical Systems, Milwaukee, WI).

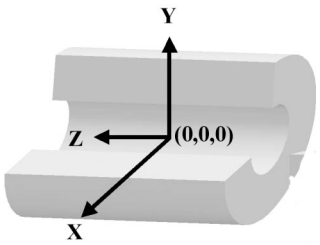

The coordinate system shown above references the MR system used for the tests in this report. Note the orientations of the MR system with respect to the direction of the coordinates, X, Y, and Z. The X=0, Y=0, and Z=0 positions, or “isocenter” is at the center of the MR system’s magnet. At this location, the magnetic field is homogeneous and the static spatial magnetic gradients are effectively zero (0). The locations indicated

in this report are referenced to this diagram (i.e., the point of the highest spatial gradient).

The test fixture was placed at the point of the highest spatial gradient for the 3-Tesla MR system. Each marker was held on the test fixture so that the string was vertical and then released. The deflection angle for each marker from the vertical direction to the nearest 1-degree was measured three times and a mean value was calculated.

Qualitative Assessment of Torque
The next evaluation of magnetic field interactions was conducted to qualitatively determine the presence of magnetic field-induced torque for each marker. This procedure involved the use of a flat plastic material with a millimeter grid on the bottom.

Each marker was placed on the test apparatus in an orientation that was 45-degrees relative to the static magnetic field of the 3-Tesla MR system. The use of 45-degree increments is deemed adequate and appropriate for a qualitative assessment of torque for an implant or device, based on reports published in the peer-reviewed literature. See reference list below. The test apparatus with each marker was then positioned in the center of the MR system, where the effect of torque from the static magnetic field is known to be the greatest, based on a previous magnetic field survey and the well-known characteristics for the 3-Tesla MR system that was used for this evaluation.

Each marker was directly observed for possible movement with respect to alignment or rotation relative to the static magnetic field of the 3-Tesla MR system. The observation process was facilitated by having the investigator inside the bore of the MR system during the test procedure. The device was then moved 45 degrees relative to its previous position and again observed for alignment or rotation.

This process was repeated to encompass a full 360 degrees rotation of positions for each marker in the 3-Tesla MR system. This procedure was conducted three times and a mean value was calculated for each marker with it orientated along its long axis and short axis.

The following qualitative scale of torque was applied to the results: 0, no torque; +1, mild or low torque, the implant slightly changed orientation but did not align to the magnetic field; +2, moderate torque, the implant aligned gradually to the magnetic field; +3, strong torque, the implant showed rapid and forceful alignment to the magnetic field; +4, very strong torque, the implant showed very rapid and very forceful alignment to the magnetic field.

Peer-reviewed, scientific publications that support performance of the test to qualitatively assess magnetic-field related torque for a metallic implant in association with an MR system are, as follows:
(1) Shellock FG, Detrick MS, Brant-Zawadzki MN. MR compatibility of Guglielmi detachable coils. Radiology 203:568-570, 1997.

(2) Shellock FG, Shellock VJ. MR-compatibility evaluation of the Spetzler titanium aneurysm clip. Radiology. 206:838-841, 1998.
(3) Shellock FG, Shellock VJ. Evaluation of cranial flap fixation clamps for compatibility with MR imaging. Radiology. 207:822-825, 1998.
(4) Shellock FG, Kanal E. Yasargil aneurysm clips: evaluation of interactions with a 1.5 Tesla MR system. Radiology. 207:587-591, 1998.
(5) Kanal E, Shellock FG. Aneurysm clips: effects of long-term and multiple exposures to a 1.5 Tesla MR system. Radiology. 210:563-565, 1999.
(6) Shellock FG, Shellock VJ. Stents: Evaluation of MRI safety. American Journal of Roentgenology. 173:543-547, 1999.
(7) Edwards, M-B, Taylor KM, Shellock FG. Prosthetic heart valves: evaluation of magnetic field interactions, heating, and artifacts at 1.5 Tesla. Journal of Magnetic Resonance Imaging. 12:363-369, 2000.
(8) Shellock FG. Surgical instruments for interventional MRI procedures: assessment of MR safety. Journal of Magnetic Resonance Imaging, 13:152-157, 2001.
(9) Shellock FG. Biomedical implants and devices: assessment of magnetic field interactions with a 3.0-Tesla MR system. Journal of Magnetic Resonance Imaging. 16:721-732, 2002.

RESULTS AND DISCUSSION

Tables 1 summarizes the results of the tests performed to determine magnetic field interactions for the markers. The mean deflection angle measured was 0-degrees for each marker relative to exposure to the 3-Tesla MR system.

This information should be considered in view of the deflection angle measurement recommendation provided by the ASTM, which states: "If the implant deflects less than 45˚, then the magnetically induced deflection force is less than the force on the implant due to gravity (its weight). For this condition, it is assumed that any risk imposed by the application of the magnetically induced force is no greater than any risk imposed by normal daily activity in the Earth's gravitational field."

Accordingly, each marker that underwent testing passed the ASTM acceptance criteria for deflection angle (i.e., less than 45 degrees of deflection) with respect to exposure to the 3-Tesla MR system used in this evaluation. Thus, these markers will not present an additional risk or hazard to a patient in the 3-Tesla MR environment with regard to translational attraction.

The qualitatively measured torque at 3-Tesla for the each marker was 0, no torque, in each case.

As such, these markers will not present an additional risk or hazard to a patient in the 3-Tesla MRI environment or less with regard to translational attraction and torque.

Importantly, because of the relatively minor translational attraction (0-degrees deflection angle) and lack of torque at 3-Tesla, it is deemed unnecessary to conduct a quantitative evaluation of torque for these markers.

MRI-Related Heating
MRI-related heating was assessed for each of the five different markers. The heating evaluation was performed according to recommendations in the following document:

F 2182–02 Standard Test Method for Measurement of Radio Frequency Induced Heating Near Passive Implants During Magnetic Resonance Imaging, ASTM International, 100 Barr Harbor Drive, PO Box C700, West Conshohocken, Pennsylvania, 19428-2959 USA.

Preparation of the Phantom. A plastic phantom was filled with a semi-solid, gelled-saline that was prepared to simulate human tissue. Gelled-saline is considered to be a more appropriate medium for the evaluation of a metallic implant versus using normal saline, alone, according to a recent publication from Park et al. (Park SM, Nyenhuis JA, Smith CD, Lim EJ, Foster KS, Baker KB, Hrdlicka G, Rezai AR, Ruggieri P, Sharan, A, Shellock FG, Stypulkowski PH, Tkach J. Gelled vs. nongelled phantom material for measurement of MRI-induced temperature increases with bioimplants. IEEE Transactions on Magnetics, 39:3367-3371, 2003.)

The plastic phantom has a configuration and dimensions to approximate the human head and torso, as follows:

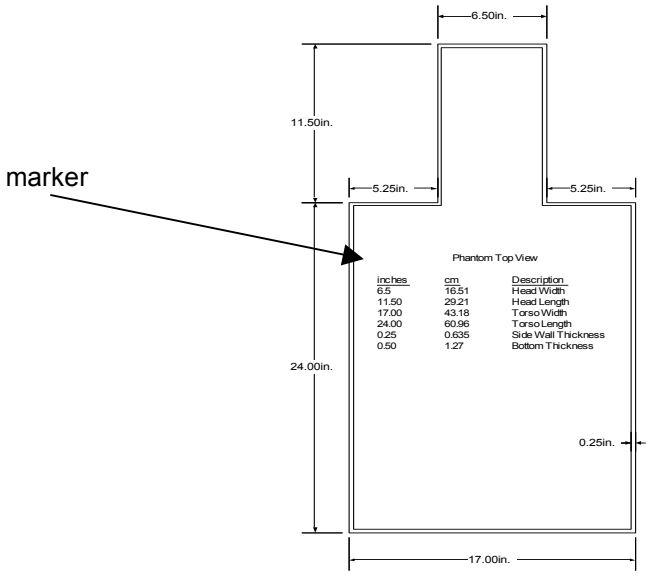

A plastic frame was placed on the bottom of the phantom along with small plastic posts to maintain the position of each marker according to its intended *in vivo* use and with regard to simulating a worst case position insofar as it is known that metallic implants

tend to heat more if closer to the inside of the MR system (i.e., thus placing it in close proximity to the transmit RF body coil).

Additional small plastic posts were placed in the plastic frame located on the bottom of the phantom to guide and maintain the positions of the fluoroptic thermometry probes used to record temperatures. This experimental set-up for the evaluation of MRI-related heating of an implant has been previously described by Rezai et al. and Finelli et al. in the peer-reviewed literature, as follows:

Rezai AR, Finelli D, Nyenhuis JA, Hrdlick G, Tkach J, Ruggieri P, Stypulkowski PH, Sharan A, Shellock FG. Neurostimulator for deep brain stimulation: Ex vivo evaluation of MRI-related heating at 1.5-Tesla. Journal of Magnetic Resonance Imaging. 15:241-250, 2002.

Finelli DA, Rezai AR, Ruggieri P, Tkach J, Nyenhuis J, Hridlicka G, Sharan A, Gonzalez-Martinez J, Stypulkowski PH, Shellock FG. MR-related heating of deep brain stimulation electrodes: an *in vitro* study of clinical imaging sequences. American Journal of Neuroradiology 23:1795-1802, 2002.

The phantom was filled with a gelling agent in an aqueous solution (i.e., 0.8-g/L NaCl plus 5.85 g/L polyacrylic acid in distilled water) to a depth of 100-mm. The mass of the phantom filled with the gelled-saline was 50-kg. Because this phantom and experimental set-up lacks “blood flow”, it further simulates an extreme condition used to assess MRI-related heating each marker.

MR System. MR imaging was performed using a 3-Tesla MR system (Excite, General Electric Medical Systems, Milwaukee, WI). The body radiofrequency (RF) coil was used to transmit and receive RF energy.

Pulse Sequence. MR imaging parameters were applied to generate a relatively high level of radiofrequency (RF) energy at 3-Tesla, as follows: spin echo pulse sequence; axial plane; repetition time, 90-msec; echo time, 8-msec; flip angle, 90 degrees; field of view, 40-cm; imaging matrix, 256 x 256; section thickness, 10-mm; number of section locations, 20; phase direction, anterior to posterior; transmitter gain, 180.

The land-marking position (i.e., the center position or anatomic region for the MR imaging procedure) and section locations were selected to encompass the entire area of the marker under evaluation. The imaging parameters produced an MR system reported value for the whole body averaged specific absorption rate (SAR) of 3.0 W/kg and spatial peak SAR of 5.8 W/kg. This level of exposure to RF energy exceeds that typically used for clinical MRI procedures.

Thermometry System. Temperature recordings were obtained in this experiment using a Luxtron Model 3100 Fluoroptic Thermometry system previously demonstrated to be MRI-compatible and unperturbed at static magnetic field strengths up to 9.0-

Tesla (an MR spectrometer). This thermometry system has small fiber-optic probes (Model SFF-2; 0.5-mm diameter) that respond rapidly (response time, 0.25 seconds), with an accuracy and resolution of ± 0.1˚C.

Thermometry Probe Placement. Each marker had thermometry probes attached to record representative temperatures during the experiment, as follows:

Probe #1, placed on one the end of the marker

In addition, a thermometry probe was placed in the phantom at a position removed (approximately 30-cm away) from the marker to record a reference temperature during the heating experiment (Probe #2).

Important Note: Because of the relatively small size of each marker only a single probe could be placed to record temperatures during the MRI-related heating assessment.

The thermometry probes were visually inspected immediately before and immediately after the MRI-heating experiment to ensure that they were properly positioned, as stated above.

Rationale for Placement of the Thermometry Probes. The fluoroptic thermometry probes were placed in contact with marker under evaluation since this is where the greatest amount of heating will occur based on prior work performed on similar implants. See the following articles that support this statement:

Nyenhuis JA, Kildishev AV, Foster KS, Graber G, Athey W. Heating near implanted medical devices by the MRI RF-magnetic field. IEEE Trans Magn 1999;35:4133–4135

Smith CD, Nyenhuis JA, Kildishev AV. Chapter 16. Health effects of induced electrical currents: Implications for implants. In: Magnetic Resonance: Health Effects and Safety, FG Shellock, Editor, CRC Press, Boca Raton, FL, 2001; pp. 393-413.

Rezai AR, Finelli D, Nyenhuis JA, Hrdlicka G, Tkach J, Sharan A, Rugieri P, Stypulkowoski PH, Shellock FG. Neurostimulation systems for deep brain stimulation: In vitro evaluation of magnetic resonance imaging-related heating at 1.5-Tesla. J Magn Reson Imaging 2002;15;241-250.

Finelli DA, Rezai AR, Ruggieri P, Tkach J, Nyenhuis J, Hridlicka G, Sharan A, Gonzalez-Martinez J, Stypulkowski PH, Shellock FG. MR-related heating of deep brain stimulation electrodes: an *in vitro* study of clinical imaging sequences. AJNR American Journal of Neuroradiology 2002;23:1795-1802.

Shellock FG. Reference Manual for Magnetic Resonance Safety, Implants and Devices: 2005 Edition. Biomedical Reference Publishing Group, Los Angeles, CA, 2005.

Protocol: The gelled-saline-filled phantom was placed in the 3-Tesla MR system and allowed to equilibrate to the environmental conditions for at least one hour. The room temperature and temperature of the bore of the MR system were 20.2˚C, with a relative humidity of 45%. The MR system fan was not on during the experiment. There was sufficient thermal equilibrium between the phantom and surrounding temperature such that the temperature of the phantom did not change by more than 0.2°C during the pre-MRI observation time for 15 minutes.

Baseline (Pre-MRI) temperatures were recorded at 10-sec. intervals for 5-minutes. MRI was then performed for 15 minutes with temperatures recorded at 10-sec. intervals. Post-MRI temperatures were recorded for 2-minutes with temperatures recorded at 10-sec. intervals. The highest temperature changes recorded for the thermometry probes are reported, herein for each marker.

RESULTS AND DISCUSSION

The results of the MRI-related heating tests are shown in Table 2. According to these data, the highest temperature changes measured for the MRI-related heating evaluation of each marker by Probe #1 was 0.5˚C in each case. The highest temperature change measured by the reference probe (Probe #2) was 0.5˚C.

Therefore, the MRI-related heating experiment for each marker at 3-Tesla using a transmit/receive body coil at a whole body averaged SAR of 3.0-W/kg and a spatial peak SAR of 5.8-W/kg indicated that was essentially no heating in association with these specific conditions, especially since the reference temperature increased 0.5˚C. This is not surprising in consideration of the relatively small size of the markers.

ARTIFACT TEST

MR imaging artifacts were assessed for the markers in association with the use of a 3-Tesla MR system. This test was accomplished by performing MR imaging with the marker placed inside of a gadolinium-doped, saline fluid-filled phantom following aspects of the American Society for Testing and Materials (ASTM) Designation: F 2119-01. Standard Test Method for Evaluation of MR Image Artifacts from Passive Implants. ASTM, West Conshohocken, PA, 2001. Gadolinium-doped, saline fluid was used for this evaluation and deemed acceptable as it provides a high signal background for the evaluation of a metallic objects and has been used in many previous MRI artifact evaluations for implants.

This test was accomplished by conducting MR imaging with the markers placed side by side inside of the gadolinium-doped, saline fluid-filled, plastic phantom (i.e., using an appropriate size relative to the size of the implant that underwent testing). There was at least 5-cm clearance between the markers and the sides of the phantom container. The markers were attached to a plastic frame to facilitate positioning and MR imaging within the phantom.

MR imaging was performed using a 3-Tesla MR system (General Electric Medical Systems, Milwaukee, WI), a send-receive RF head coil, and the following pulse sequences:

(1) T1-weighted, spin echo pulse sequence; repetition time, 500 msec; echo time, 20 msec; matrix size, 256 X 256; section thickness, 5-mm; field of view, 24-cm; number of excitations, 2; bandwidth; 16 kHz
(2) Gradient echo (GRE) pulse sequence; repetition time, 100 msec; echo time, 15 msec; flip angle, 30 degrees; matrix size, 256 X 256; section thickness, 5-mm; field of view, 24-cm; number of excitations, 2; bandwidth, 16 kHz

These are commonly used pulse sequences for MR imaging. In addition, the GRE pulse sequence is a gradient echo or partial flip angle technique that tends to have a great degree of artifact associated with it when MR imaging is performed on a metallic implant. Thus, the use of the GRE pulse sequence represents a type of extreme MR imaging condition.

The imaging planes were oriented to encompass the long axis and short axis of the markers. The frequency encoding direction was parallel to the plane of imaging. Notably, the image locations obtained through the markers were selected from multiple "scout" MR images to represent the largest or worst-case artifacts.

Artifacts that result from other positions of the imaging plane relative to the markers or with regard to the particular orientation of the implant to the main magnetic field of the MR system may be slightly more or less to that observed under the experimental conditions used in the test for artifact assessment. Nevertheless, the MR imaging technique used to assess artifacts is the same as that published in the peer-reviewed literature (see list below). For this reason, it was selected to assess the markers since it is considered appropriate and facilitates comparison to previously evaluated metallic implants.

Artifacts were characterized using a previously-published methodology described in the following publications:
(1) Shellock FG, Shellock VJ. MR-compatibility evaluation of the Spetzler titanium aneurysm clip. Radiology. 206:838-841, 1998.
(2) Shellock FG, Shellock VJ. Evaluation of cranial flap fixation clamps for compatibility with MR imaging. Radiology. 207:822-825, 1998.
(3) Edwards, M-B, Taylor KM, Shellock FG. Prosthetic heart valves: evaluation of magnetic field interactions, heating, and artifacts at 1.5 Tesla. Journal of Magnetic Resonance Imaging. 12:363-369, 2000.
(4) Shellock FG. Surgical instruments for interventional MRI procedures: assessment of MR safety. Journal of Magnetic Resonance Imaging, 13:152-157, 2001.

The planimetry software provided with the MR system was used to measure the cross-sectional areas for the artifacts associated with the markers. The accuracy of this measurement method is ± 10%. MR images are provided showing the artifacts.

Important Note: Due to the extremely small size of the markers, this level of accuracy may not be adequate for proper measurements. As such, qualitative criteria were also applied to the results to provide information pertaining to the relative sizes of the artifacts.

Thus, measurements were obtained to determine the maximum or worst case artifact area related to the presence of the markers for each MR imaging condition. Notably, this ensured that the artifacts for the markers were not underestimated.

RESULTS AND DISCUSSION

Artifact test results are indicated in Table 3 of this report and shown on the enclosed figures displaying the MR images that were obtained. In general, the artifacts that appeared on the MR images were shown as a localized signal voids (i.e., signal loss) that were minimal in size relative to the size and shape of the markers.

The gradient echo pulse sequence produced larger artifacts than the T1-weighted, spin echo pulse sequence for each marker. Test Article #1 showed the least amount of artifact, while Test Article #4 showed the greatest amount of artifact.

SUMMARY

Based on the MR testing information, it appears that these five different markers will not present an additional hazard or risk to a patient undergoing an MRI procedure using a scanner operating with a static magnetic field of 3-Tesla or less and under the MRI-related heating conditions used for this evaluation. Artifacts for these markers vary according to the size and shape of the respective marker as stated above.

IMPORTANT NOTE: If you plan to submit this information to the United States Food and Drug Administration to obtain a labeling claim of "MR-safe" or other similar labeling, please provide me with the content to review to ensure proper presentation of the information.

Table 1. Evaluation of magnetic field interactions for the five different markers.

Test Article 1 Carbon coated zirc. Oxide 0.121 x 0.054 inch Breast Tumor Marking

	Deflection Angle (degrees)	Torque long axis	Torque short axis
Measurement #1	0	0	0
Measurement #2	0	0	0
Measurement #3	0	0	0

Deflection Angle (degrees, m ± SD)	Torque (m ± SD) long axis	Torque (m ± SD) short axis
0 ± 0	0 ± 0	0 ± 0

Test Article 2 Carbon coated zirc. Oxide 0.121 x 0.054 inch Breast Tumor Marking

	Deflection Angle (degrees)	Torque long axis	Torque short axis
Measurement #1	0	0	0
Measurement #2	0	0	0
Measurement #3	0	0	0

Deflection Angle (degrees, m ± SD)	Torque (m ± SD) long axis	Torque (m ± SD) short axis
0 ± 0	0 ± 0	0 ± 0

Test Article 3 Carbon coated zirc. Oxide 0.182 x 0.079 inch Breast Tumor Marking

	Deflection Angle (degrees)	Torque long axis	Torque short axis
Measurement #1	0	0	0
Measurement #2	0	0	0
Measurement #3	0	0	0

Deflection Angle (degrees, m ± SD)	Torque (m ± SD) long axis	Torque (m ± SD) short axis
0 ± 0	0 ± 0	0 ± 0

Test Article 4 Carbon coated zirc. Oxide 0.182 x 0.079 inch Breast Tumor Marking

	Deflection Angle (degrees)	Torque long axis	Torque short axis
Measurement #1	0	0	0
Measurement #2	0	0	0
Measurement #3	0	0	0

Deflection Angle (degrees, m ± SD)	Torque (m ± SD) long axis	Torque (m ± SD) short axis
0 ± 0	0 ± 0	0 ± 0

Control 1 Titanium alloy 0.080 x 0.050 inch Breast Tumor Marking

	Deflection Angle (degrees)	Torque long axis	Torque short axis
Measurement #1	0	0	0
Measurement #2	0	0	0
Measurement #3	0	0	0

Deflection Angle (degrees, m ± SD)	Torque (m ± SD) long axis	Torque (m ± SD) short axis
0 ± 0	0 ± 0	0 ± 0

Table 2. Summary of MRI-related heating results for the five different markers.

Marker	Probe 1 Highest Temp. Change (˚C)	Probe 2 Highest Temp. Change (˚C)	Probe 3 Highest Temp. Change (˚C)
Test Article 1	0.5	0.5	0.5
Test Article 2	0.5	0.5	0.5
Test Article 3	0.5	0.5	0.5
Test Article 4	0.5	0.5	0.5
Control 1	0.5	0.5	0.5

Table 3. Summary of MRI artifact information for the implants.

Test Article 1, Carbon coated zirc. Oxide, 0.121 x 0.054 inch				
Signal Void Size (mm^2)	2	3	9	14
Test Article 2, Carbon coated zirc. Oxide, 0.121 x 0.054 inch				
Signal Void Size (mm^2)	13	17	34	33
Test Article 3, Carbon coated zirc. Oxide, 0.182 x 0.079 inch				
Signal Void Size (mm^2)	17	17	34	38
Test Article 4, Carbon coated zirc. Oxide, 0.182 x 0.079 inch				
Signal Void Size (mm^2)	58	62	127	117
Control 1, Titanium alloy, 0.080 x 0.050 inch				
Signal Void Size	8	2	9	18
Pulse Sequence	T1-SE	T1-SE	GRE	GRE
Static Magnetic Field (T)	3	3	3	3
TR (msec.)	500	500	100	100
TE (msec.)	20	20	15	15
Flip Angle	N/A	N/A	30˚	30˚
Bandwidth	16 kHz	16 kHz	16 kHz	16 kHz
Field of View	24 cm	24 cm	24 cm	24 cm
Matrix Size	256 x 256	256 x 256	256 x 256	256 x 256
Section Thickness	5 mm	5 mm	5 mm	5 mm
Imaging Plane	parallel	perpendicular	parallel	perpendicular
	(long axis)	(short axis)	(long axis)	(short axis)
Phantom Filler	fluid	fluid	fluid	fluid

(T1-SE, T1-weighted spin echo; GRE, gradient echo; N/A, not applicable)

FIGURE 1. The five different markers that underwent testing for magnetic resonance (MR) safety and artifacts at 3-Tesla.
(Left to Right)
Test Article 1, Carbon coated zirc. Oxide
Test Article 2, Carbon coated zirc. Oxide
Test Article 3, Carbon coated zirc. Oxide
Test Article 4, Carbon coated zirc. Oxide
Control 1, Titanium alloy

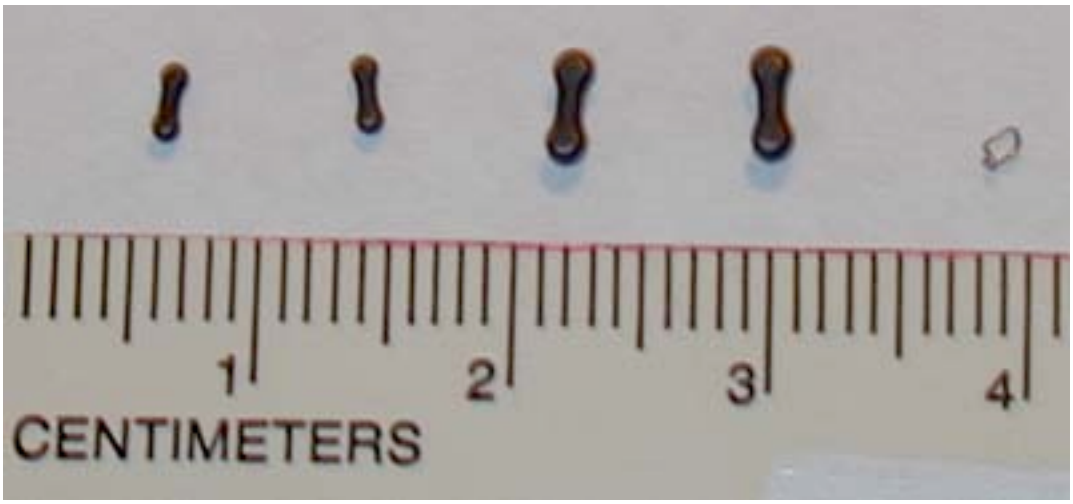

FIGURE 2. The 3-Tesla MR system (Excite, General Electric Medical Systems, Milwaukee, WI) used for the assessment of MR safety and artifacts for the markers.

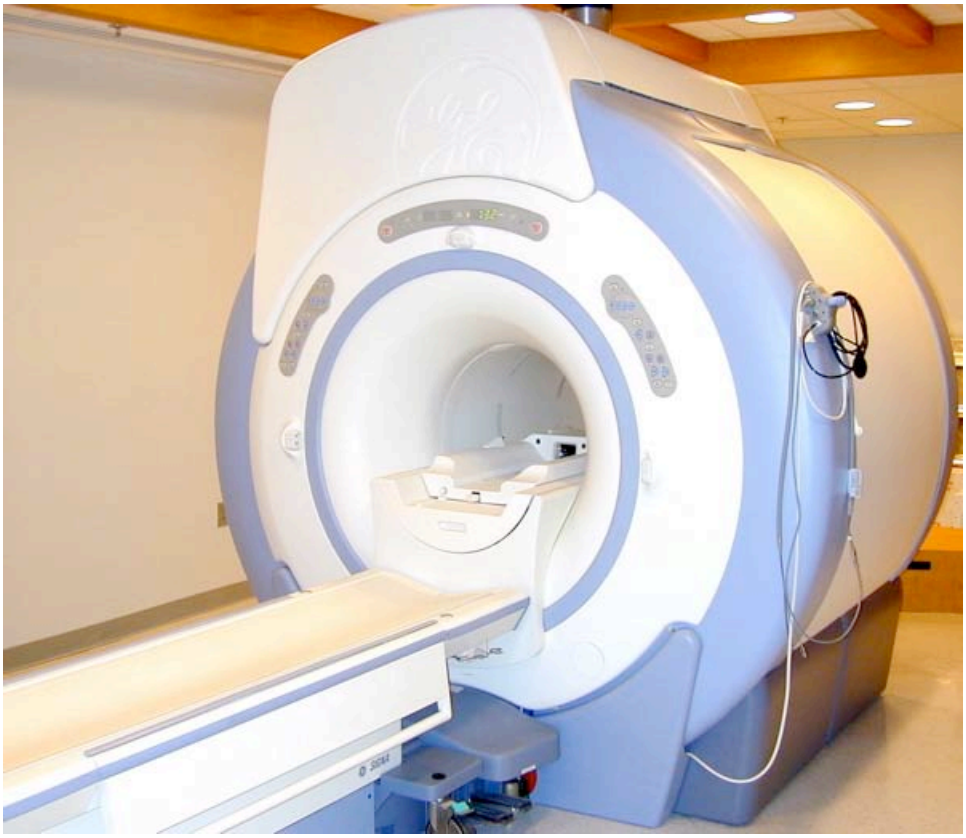

FIGURE 3. The deflection angle test conducted at 3-Tesla on markers (no photo available for Control 1, Titanium alloy). Note the deflection angle of 0-degrees measured in the 3-Tesla scanner at the point of the highest spatial gradient in each case. (Top to bottom, Test Article 1, Test Article 2, Carbon coated zirc. Oxide Test Article 3, Test Article 4).

FIGURE 4. Example showing position for the fluoroptic thermometry probe relative to the marker used to record temperatures during the MRI-related heating experiments performed at 3-Tesla.

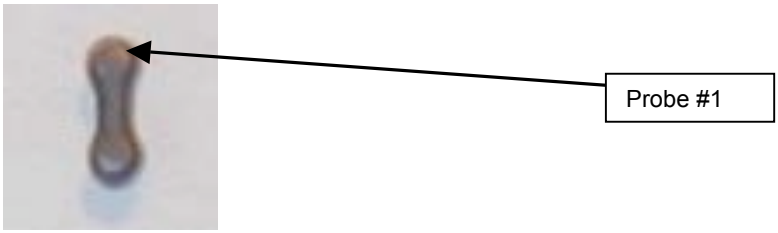

FIGURE 5. Experimental set up showing the 3-Tesla MR system and head/torso phantom used for the evaluation of MRI-related heating for the markers. Note the cables going to the fluoroptic thermometry probes of the Luxtron system.

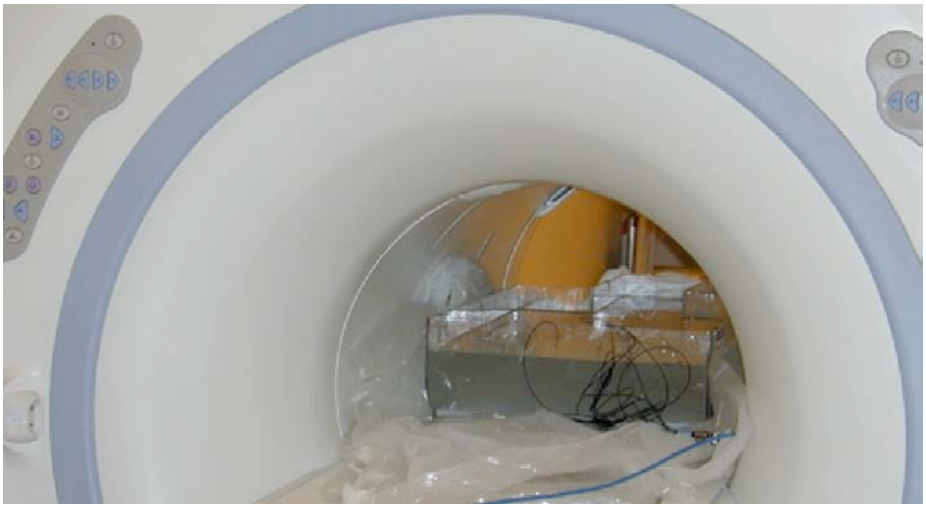

FIGURE 6. Experimental set-up used to evaluate artifacts for the markers at 3-Tesla.

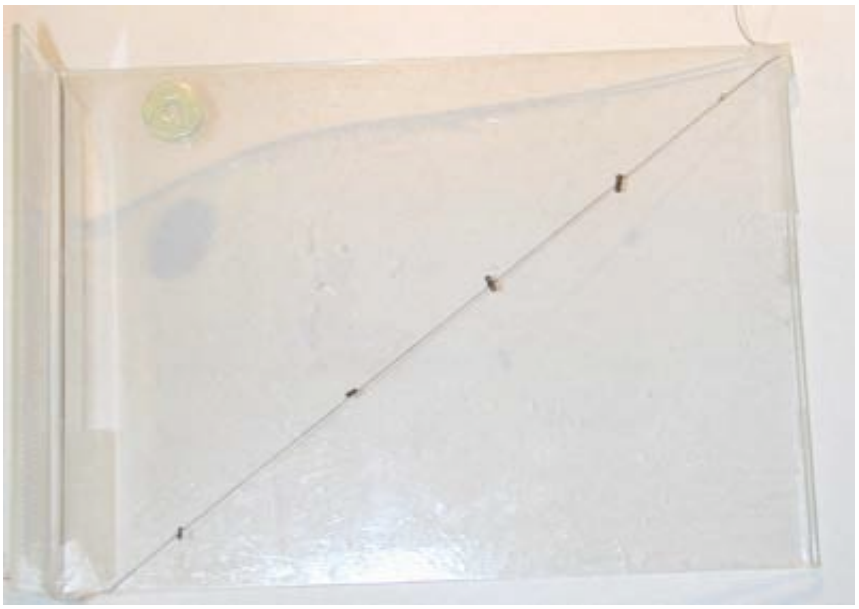

Plastic grid with markers, left to right, Test Article 1, Test Article 2, Test Article 3, Test Article 4, Control 1, Titanium alloy

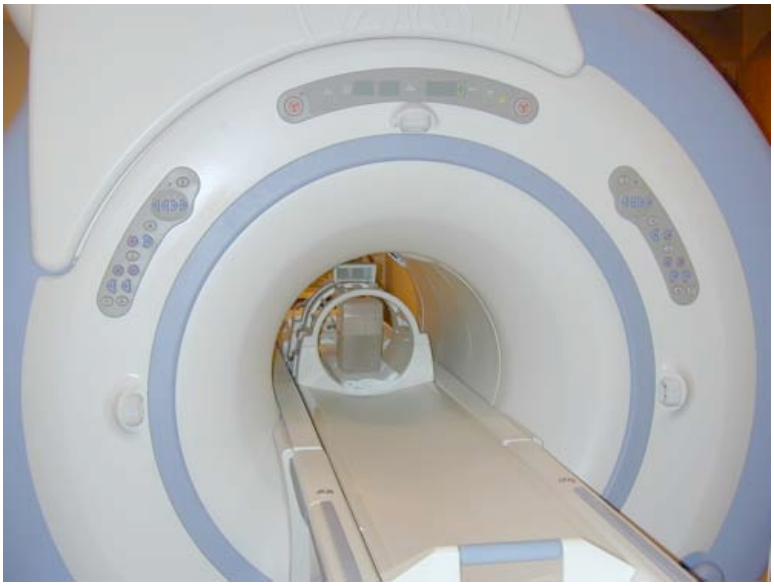

Fluid-filled phantom with the markers inside of the head RF coil in the 3-Tesla MR system.

FIGURE 7. T1-weighted, spin echo pulse sequence; long axis imaging plane Markers #1, #2, #3, #4, C (control).

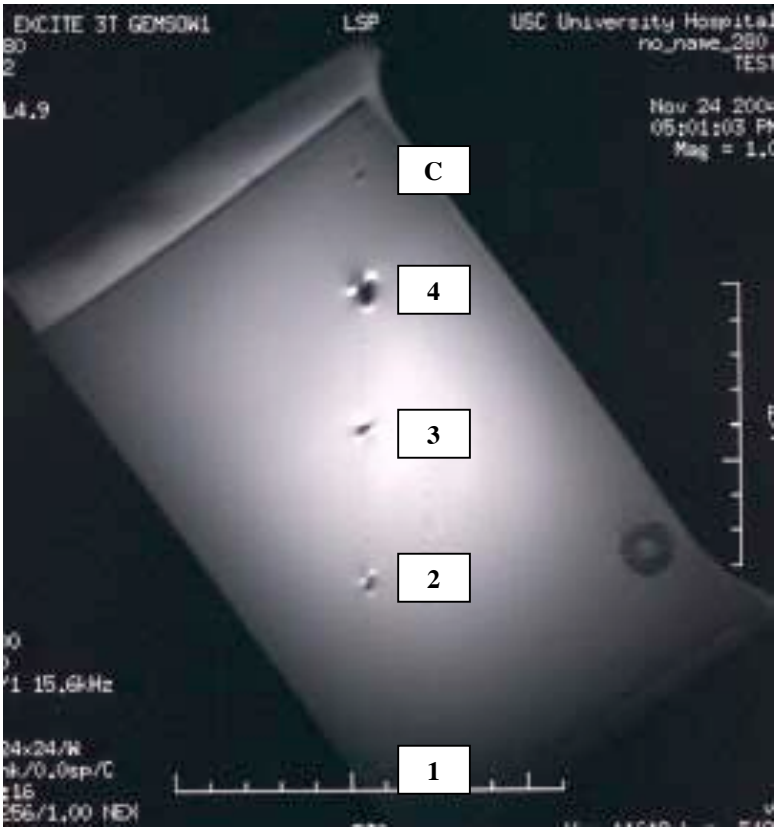

FIGURE 8. T1-weighted, spin echo pulse sequence; short axis imaging plane Markers #1, #2, #3, #4, C (control).

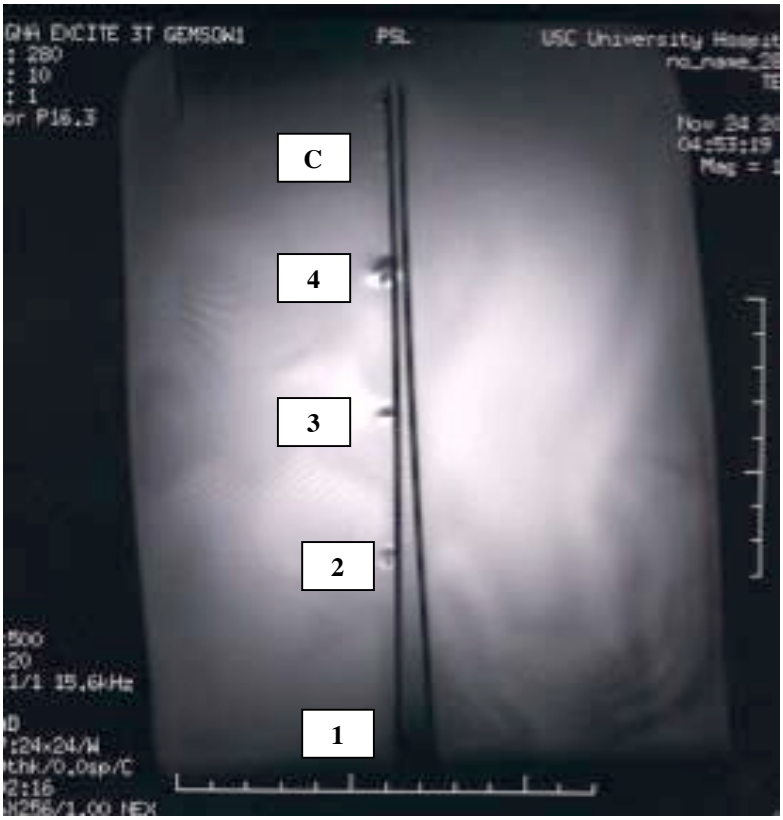

FIGURE 9. Gradient echo pulse sequence; long axis imaging plane

Markers #1, #2, #3, #4, C (control).

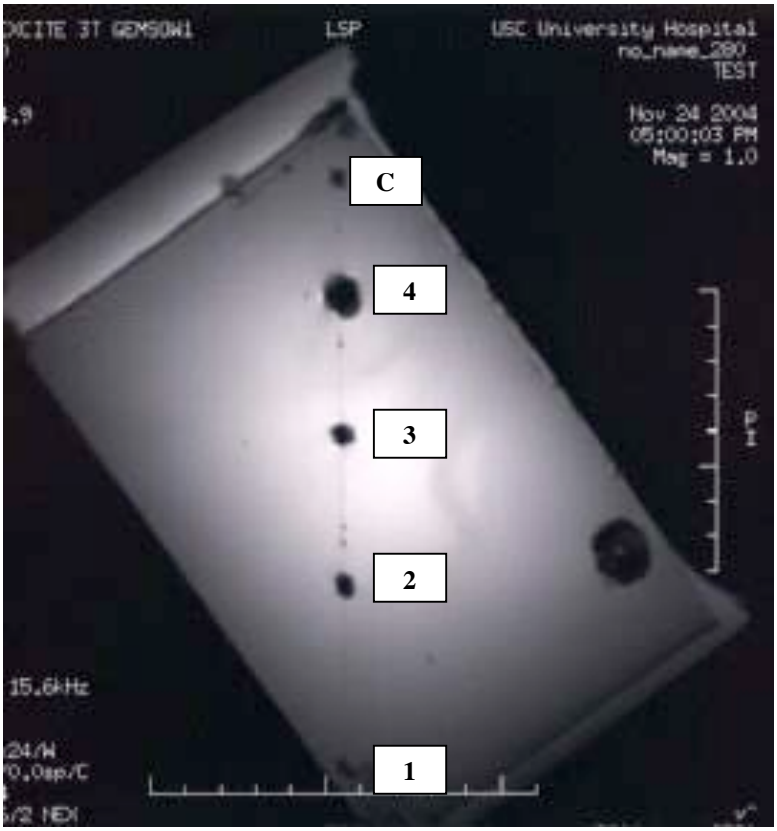

FIGURE 10. Gradient echo pulse sequence; short axis imaging plane

Markers #1, #2, #3, #4, C (control)